horticulturae

MDPI

Article

Evaluation of Statistical Models of NDVI and Agronomic Variables in a Protected Agriculture System

Edgar Vladimir Gutiérrez-Castorena *, Joseph Alejandro Silva-Núñez, Francia Deyanira Gaytán-Martínez, Vicente Vidal Encinia-Uribe, Gustavo Andrés Ramírez-Gómez and Emilio Olivares-Sáenz

Facultad de Agronomía, Universidad Autónoma de Nuevo León, Francisco I. Madero S/N, Ex. Hacienda el Canadá, General Escobedo 66050, Mexico; joseph.silvanu@uanl.edu.mx (J.A.S.-N.); francia.gaytanmrt@uanl.edu.mx (F.D.G.-M.); vicente.enciniaur@uanl.edu.mx (V.V.E.-U.); gustavo.ramirezgmz@uanl.edu.mx (G.A.R.-G.); emilio.olivaressn@uanl.edu.mx (E.O.-S.)
* Correspondence: edgar.gutierrezcs@uanl.edu.mx

Abstract: Vegetable production in intensive protected agriculture systems has evolved due to its intensity and economic importance. Sensors are increasingly common for decision-making in crop management and control of environmental variables, obtaining optimal yields, such as estimating vegetation indices. Innovation and technological advances in unmanned vehicle platforms have improved spatial, spectral, and temporal resolution. However, in protected agriculture systems, the use is limited due to the assumption of having controlled environmental conditions for indeterminate vegetable production. Therefore, sequential monitoring of NDVI is proposed during the 2022 and 2023 agricultural cycles using the Green Seeker® sensor and agronomic variables. This has created a database to generate predictive models of development and yield as a function of nutrient status. The results obtained indicate high significance levels for the development and NDVI curves in all phenological stages; in contrast to the yield predictive models, this is due to the maximum values (close to one) recorded for NDVI inside the greenhouse in comparison to the yield prediction obtained from the 18th week of harvest. Evaluating the models between NDVI and agronomic variables is not an index that offers certainty in predicting yield in indeterminate crops in protected agriculture production systems. This is due to the constant optimal development in response to controlled environmental conditions, nutrient status, and water supply inside the greenhouse, without the sustainability of yield, which decreases in the final stages of production until production becomes economically unprofitable.

Keywords: Green Seeker®; predictive models; greenhouse; indeterminate crops

Academic Editors: Chenglin Wang, Lufeng Luo, Juntao Xiong and Xiangjun Zou

Received: 12 December 2024
Revised: 18 January 2025
Accepted: 23 January 2025
Published: 26 January 2025

Citation: Gutiérrez-Castorena, E.V.; Silva-Núñez, J.A.; Gaytán-Martínez, F.D.; Encinia-Uribe, V.V.; Ramírez-Gómez, G.A.; Olivares-Sáenz, E. Evaluation of Statistical Models of NDVI and Agronomic Variables in a Protected Agriculture System. *Horticulturae* **2025**, *11*, 131. https://doi.org/10.3390/horticulturae11020131

1. Introduction

Protected agriculture is an agricultural production technique that provides controlled conditions of temperature, humidity, CO_2 concentration, airflow, radiation, irrigation, and nutritional status of the crop, avoiding physiological affectations due to environmental adversities or attacks by pests and diseases, achieving optimal yields compared to air-field production [1]. External and internal factors present a changing interrelationship in a short time and region. Such is the case between the speed and direction of the wind from outside and the temperature and relative humidity distributions inside due to the internally forced airflow; the higher the flow, the lower the temperature and the higher the relative humidity [2]. Alternatively, lowering indoor temperature by evaporative cooling with forced ventilation provides optimal conditions at the cost of rapid deterioration in ventilation systems [3] or the correct application of irrigation as the main factor affecting

crop yield [4], understanding that yield is determined by the ability to accumulate dry matter in organs, of which some factors have limited the production system due to poor planning on agronomic management, soil, and water contamination, excessive use of synthetic fertilizers, or economic implications mainly due to excessive energy consumption [5]. One of the main issues identified in the literature is the high cost of multispectral images from satellite platforms, as well as their low capture frequency, which limits their use in scenarios requiring a faster response, such as nutrient and irrigation management [6]. Furthermore, to date, few studies have employed direct NDVI measurements to quantify the yield stability of common wheat, thereby constraining selection efficiency and our understanding of specific phenotypic adaptations in the target environment [7].

To avoid production decreases, producers have implemented sequential monitoring strategies for efficient water use, involving the nutritional status of the crop through the application of synthetic fertilizers in irrigation [8], which has been modified from the type of intensive agricultural production system considered high-tech [9], to obtain optimal yields in each cycle, of which the economic is not a constraint. To this end, agronomic management is being implemented with the use of remote sensing of digital images on various observation platforms in unmanned aerial vehicles [10] with the purpose of quantifying agronomic variables [11]. One of them is the radiation absorbed and reflected by the cultivars at various wavelengths of the visible electromagnetic spectrum of the RGB or near-infrared image [12]; other managements refer to the integral monitoring of soil components [13], irrigation monitoring [14], or biophysical and biochemical changes, which together provide results for the timely detection of nutritional anomalies in soil development crops [15,16].

Five decades ago, digital sensors were developed and implemented to assess plant cover, soil moisture, and surface radiant temperature as microclimatic variables [17] that, through statistical analysis, can predict future values due to the initial characteristics of the surface. Given the current technological development of sensors, the autonomous recording of microenvironmental values has been implemented in a timely and specific manner in the vegetable production system, in addition to implementing strategies in the usual disease detection methods to reduce time and resources through automatic detection as a complementary tool to determine crop health [18]. The goal is to generate greater food production per unit of surface area, which the protected agriculture system takes for granted by restricting and limiting entry with anti-aphid nets. However, these agronomic management practices are neither unique nor exclusive. To this end, actions have been established to promptly identify foliar chlorosis caused by some nutrient deficiencies in plants in real time, which is essential to optimize the use of fertilizers [19]. Since obtaining nutritional information in a standard assessment still faces challenges due to the difficulty of identifying deficiencies in both species and environments, RGB image analysis processes have been proposed from sensors on satellite platforms [20] and unmanned aerial vehicles (UAVs) [21]. However, imaging technology to monitor specific phenotypic changes (from leaf to canopy) related to plant feeding during development is limited, even more so in obtaining adequate spectral information to track chemical components in plants directly. References [19,22,23] point out that climatic variability influences accelerated crop growth, resulting in differences in the different crop stages within the same productive cycle, limiting yield estimation due to the wide range of NDVI values. Yield models based on linear regressions that use NDVI as a predictor have been applied to crops such as rice and wheat [24], as well as maize [25]. For these purposes, different types of sensors have been employed, including those attached to unmanned vehicles (UAFs), mounted on tractors, or used manually. The latter instrumentation allows continuous and point measurements in the field, which provides information on soil and vegetation characteristics at less than 2 m

distance with respect to the object [25], counteracting the drawbacks of sensors at higher altitudes [26–28] used to perceive changes in land use or changes in vegetation through vegetation indices [29] at different scales of observation [30].

Vegetation indices indicate the components of vegetation cover on the land surface [31] or identify the crop type [11]. However, it depends on specific characteristics, such as sensor tilt angle, focal length, measurement hours [32], or the type of sensor to obtain the digital image and thus generate the statistical models. The Normalized Difference Vegetation Index (NDVI) is the most used indicator because it denotes permutations in vegetation, with better statistical certainty in relation to the nutrient status of the plant [33], with different moisture gradients in unmanned vehicles [34], in great diversity and numerical variability of crops [35], or even more, employed in the elaboration of thematic maps of vegetative development graphically between the relationship of NDVI with agronomic variables at ambient temperature [36].

Currently, there are proximity sensors with the ability to obtain NDVI without the atmospheric drawbacks recorded by satellite platforms, such as Crop Circle ACS [37], RapidScan CS-45 (Holland Scientific Inc., Lincoln, NE, USA) [38], and finally, Green Seeker® [39,40], which solved the atmospheric interference problem [41] by possessing their own emission source (light-emitting diodes) that replaces the radiation emitted by the sun [42]. However, these, in turn, register limiting factors of focal distance, tilt angle, and inference with other components of the study area, affecting the index with another type of plant without economic importance [43] or environmental irradiation in specific conditions [40], or coupling to mobile platforms [44] without affectation by the incidence of artificial light [45].

On the other hand, in Mexico, 6.82% of the agricultural area (31,191.39 ha) is under some protected agriculture system, of which 7300.00 ha are used for greenhouse tomato cultivation, with an average annual yield of 1.35 M tons, of which the state of Nuevo León contributes 25,000 tons distributed over 112 ha [46]. To this end, the private initiative, state government, and small producers formalized alliances with the various sectors and socioeconomic levels of the population, creating models of social entrepreneurship called Agroparques horticultural with an entrepreneurial vision (Secretaria de Desarrollo Agropecuario). This partnership has led to a steady expansion of the tomato production system in protected agriculture systems directly in soil or semi-hydroponics.

The food production system through protected agriculture has constantly implemented new and innovative technologies with multidisciplinary tools, artificial intelligence, or the use of the internet to communicate neural networks in low-power areas [47], focusing on intensive vegetable production with sustainable development. However, detecting and timely correcting adverse factors such as soil moisture, water stress, ambient temperature, and light intensity involves specific studies and techniques of consecutive sequential monitoring to obtain optimal production yields.

Some innovations carried out are aimed at determining crop evapotranspiration (ET), with improvements in simulation accuracy to optimize fertigation and water resource saving [48] to avoid water stress as a sign of root system functions [49], providing irrigation doses and frequencies to obtain good yields and fruit quality [50], all focused on the sequential monitoring of nutrient uptake, phyto-sensing, smart technologies, and sustainability of water and nutrient supply by crops [51] by using real-time sensors inside the greenhouse at a commercial scale [52].

Monitoring the nutritional status of the indeterminate crop in real time with proximity sensors must include phenological phases and historical yield data, with the purpose of establishing the end-of-harvest date due to the continuous vegetative development, which is challenging to identify in the field with vegetation indices. Therefore, establish-

ing it requires a previous instrumental calibration, specific conditions of the production system, agronomic management, temperature, and humidity, as well as crop variety because they reveal a leaf area index by the differential percentage of sunlight in the photosynthetic capacity [53].

To this end, specific crop management techniques have been proposed, such as stem management to influence plant physiology, yield, and fruit quality [54,55] by stopping the indeterminate development of the plant or after a limited number of bunches by cutting the terminal bud of the plant [56], or modification of the crop canopy architecture as a central component of yield. Consequently, the present research proposes generating growth and yield estimation models by correlating NDVI values (Green Seeker®) and agronomic variables from the generation of databases at different stages of the indeterminate-type tomato crop established in an intensive protected agriculture production system.

2. Materials and Methods

2.1. Study Area

The experiment was set up in a semi-automatic greenhouse of the Israelite type without forced ventilation in an area of 1000 m^2; the fertigation system consists of water flow doses by tape. The soil preparation (Figure 1a) consists of semi-conventional tillage (subsoiling, plowing, and harrowing every 3 agricultural cycles) and tillage with roto-cultivation; the border is of the seedbed type; the varieties of indeterminate tomato (*Solanum lycopersicum* L.) were ¨El Potosí¨ of the saladette type and ¨El Arameo¨ of the beef type (Figure 1b). Seed propagation was carried out in propagation trays, with transplanting 35 days after sowing; the seedling was treated with fungicide (carbendazim), insecticide (imidacloprid) and fertilizer (propamocarb hydrochloride) in doses of 1, 1.5, and 1 mL L^{-1}, respectively, as well as 1 g L^{-1} of 12-43-12 fertilizer (to the seedling root beef) in 10 L of water.

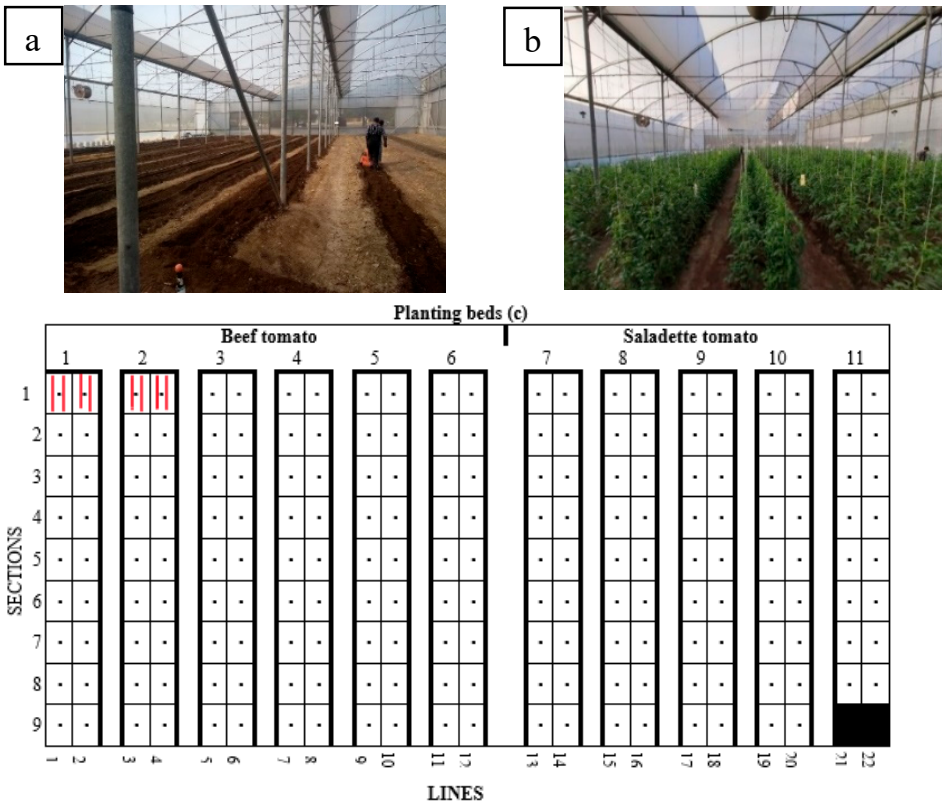

Figure 1. (**a**) Bed preparation with a rototiller; (**b**) developed tomato plants; (**c**) distribution diagram of beds, lines, sections, and average points of NDVI by sensor sweep of a set of plants per section (example: 1, 1) (north—south longitudinal direction).

2.2. Sampling Sites

The greenhouse was divided into 11 beds (1.80 m from center to center); each bed was subdivided into nine sections (3.8 m long) with planting in double lines in the north–south direction (Figure 1c). Systematic sampling was carried out, giving a point value of NDVI central to the section, from the sweep of readings (plant line, section, and bed) obtaining 198 data per week, in addition to selecting plants at random per section to record agronomic variables throughout the agricultural cycle, such as plant height (PH), leaf length (LL), leaf width (LW), stem diameter (SD), number of clusters (NC), and number of fruits (NF).

2.3. Sensor Calibration

The sensor calibration consisted of monitoring the tomato crop established in a 5 m long strip in a controlled environment by sweeping it every 15 days, with inputs of foliar fertilization of macro- and microelements during the development stages until the first products.

According to the operator's manual [57], maintaining measurement accuracy involves keeping a consistent distance above the crop canopy to avoid variations in the fraction of light reflected back to the sensor—this distance depends on the extent of the plant's coverage—positioning the sensor parallel to the ground and directly toward the crop to ensure uniform light capture, avoiding any tilt or inclination, moving the sensor at a steady pace to prevent abrupt changes that might affect data collection, recording the precise location of each measurement for easier comparison at various growth stages, and using supports when crops exceed the operator's height to maintain the proper distance between the sensor and the plant surface. In this last case, a reference point should be marked to ensure consistency; for indeterminate tomato crops, a clearance of 60 cm is recommended.

2.4. Normalized Differential Index (NDVI)

A database was generated with the information obtained from NDVI values acquired by the Green Seeker® TM optical sensor (Model HCS-100, 2012, Trimble Inc., Sunnyvale, CA, USA). Systematic monitoring was initiated 5 days after transplanting, repeated every 7 days, and ended 211 days later (28 weeks). NDVI values were plotted on thematic maps using the simple Kriging method of plant growth between beds and yield per section.

2.5. Statistical Analysis

The statistic used to evaluate the NDVI values of the tomato crop by beds, section, line, and week of development after transplanting was an analysis of variance (ANOVA) and Tukey's comparison of means; in addition, a Pearson correlation matrix was performed to estimate the relationship between the agronomic variables of the plant and the reflectivity values. Finally, multiple regression predictive models were created to create a development curve and a predictive yield model by beds using the values of the variables obtained during sampling. The proposed multiple regression model with successive steps allows only statistically significant variables to be included in the equation.

The base formula is as follows:

$$Yi = \beta 0 + \beta 1X1i + \beta 2X2i + \ldots + \beta nXni + ei \; i = 1, 2, \ldots n$$

where

- Yi: dependent variable;
- $\beta 0$: constant of the ordinate of origin;
- βn: partial coefficients in the regression;
- Xni: sampled agronomic variable (PH, LL, etc.);
- ei: uncontrolled error.

2.6. Vegetation Index Thematic Maps

NDVI thematic maps were created using qGis v.3.38.2 software and the simple Kriging method. This allows for calculating a specific point's value based on neighboring points' values. Each section is represented by the average NDVI value readings on a color scale ranging from 0.0 (red color) to a shade of dark green (representing values close to 1), through orange and yellow for average values (at 0.05 intervals). At the same time, yield values were extracted in kg per week for each bed, being classified as no yield (no color), 0.0–39.9 kg (green), 40–79.9 kg (blue), and 80 kg (red). In addition, all values were used to correlate NDVI with yield in both varieties of tomato.

3. Results and Discussion

3.1. Statistic Study

ANOVA statistics, Pearson's correlation, and comparison of means were performed on a database with 17,500 values of NDVI and agronomic variables obtained weekly (15 days after transplanting) for 28 consecutive weeks during the entire agricultural cycle. The analysis of variance shows the variability of NDVI values by bed, section, and week, which denotes the heterogeneity of the plants even when maintained in an intensive production system in a controlled environment and agronomic management, which reports a statistically significant difference ($p < 0.05$) for both the beef and saladette tomato varieties at the bed, section, and time (week of development) scales (Table 1).

Table 1. Analysis of variance (ANOVA) of NDVI in beef and saladette tomato by bed, section, and week.

	Beef Tomato		Saladette Tomato	
Components	**Sum of Squares**	**Significance**	**Sum of Squares**	**Significance**
Planting bed	1.370	0.000	1.059	0.000
Section	0.294	0.000	0.595	0.000
Week	11.387	0.000	10.653	0.000
Error	3.807		6.176	
Total	16.857		18.532	

Regarding the means by Tukey's method, a statistically significant difference ($p = 0.05$) was detected between beds, of which beds 1 and 2 in the beef tomato variety reported high NDVI values that ranged between 0.71 and 0.69, respectively. Meanwhile, in saladette tomato varieties, beds 8 and 11 had index values between 0.66 and 0.65, motivated by higher soil moisture supplied in irrigations during the first weeks, which favored crop development, contrary to the values recorded in bed 7, which registered a lower canopy cover, and therefore, the index was lower during the experiment, with a value of around 0.57 (Table 2).

The comparison of NDVI means between sections does not show a statistically significant difference ($p = 0.05$) (Table 3). However, the first three sections in both varieties have the highest means in response to the greater amount of water available at the time of irrigation due to a combination of factors, such as the slope of the land and water flow.

The correlation coefficient between variables (Table 4) evidenced the relationships with influence on the NDVI value, which are plant length with R = 0.81 between the beef variety tomato and R = 0.93 between the saladette variety tomato. With respect to the leaf width variables, the value reported was R = 0.75 between the beef variety tomato and R = 0.89 for the saladette variety tomato. This is due to the plant alveolus with greater plant cover.

Table 2. Comparison of NDVI means between beds using Tukey's method.

Beef Tomato						Saladette Tomato				
Planting Bed	N	Subset				Planting Bed	N	Subset		
		a	b	c	d			a	b	c
6	252	0.61 a				7	252	0.57 a		
5	252		0.65 b			10	252		0.62 b	
3	252		0.66 b			9	252		0.63 b	
4	252		0.67 bc	0.67 bc		11	208		0.65 bc	0.65 bc
2	252			0.69 cd	0.69 cd	8	252			0.66 c
1	252				0.71 d					
					Alpha = 0.05					

Note: a, b, c, and d = subsets; N = number of samplings of each during the 28 weeks.

Table 3. Tukey mean comparison of NDVI.

Beef Tomato					Saladette Tomato				
Section	N	Subset			Section	N	Subset		
		a	b	c			a	b	c
8	168	0.64 a			5	138	0.59 a		
6	168	0.65 ab	0.65 ab		8	138	0.61 ab	0.61 ab	
7	168	0.66 abc	0.66 abc	0.66 abc	6	138	0.61 ab	0.61 ab	
9	168	0.67 abc	0.67 abc	0.67 abc	7	138	0.62 abc	0.62 abc	0.62 abc
5	168	0.67 abc	0.67 abc	0.67 abc	4	138	0.62 abc	0.62 abc	0.62 abc
4	168	0.67 abc	0.67 abc	0.67 abc	9	112	0.64 abc	0.64 abc	0.64 abc
1	168	0.68 abc	0.68 abc	0.68 abc	2	138		0.65 abc	0.65 abc
3	168		0.68 bc	0.68 bc	1	138		0.65 abc	0.65 abc
2	168			0.69 c	3	138			0.66 c
				Alpha = 0.05					

Note: a, b, c = subsets, N = number of samplings of each bed during the 28 weeks.

Table 4. Pearson correlation matrix between values of agronomic variables and NDVI for beef and saladette tomato.

		Beef Tomato							Saladette Tomato						
		PH	LL	LW	SD	NC	NF	NDVI	PH	LL	LW	SD	NC	NF	NDVI
PH	R	**1**	0.19	0.38	0.91	−0.22	−0.28	0.29	**1**	0.27	0.41	0.90	−0.16	−0.17	0.33
	Sig.		0.31	0.04	0.00	0.33	0.21	0.12		0.08	0.02	0.00	0.24	0.23	0.04
LL	R	0.19	**1**	0.96	0.52	0.29	0.36	0.81	0.27	**1**	0.98	0.60	0.43	0.44	0.93
	Sig.	0.31		0.00	0.00	0.21	0.11	0.00	0.08		0.00	0.00	0.03	0.03	0.00
LW	R	0.38	0.96	**1**	0.65	0.35	0.45	0.75	0.41	0.98	**1**	0.68	0.46	0.47	0.89
	Sig.	0.04	0.00		0.00	0.12	0.04	0.00	0.02	0.00		0.00	0.02	0.02	0.00
SD	R	0.91	0.52	0.65	**1**	−0.00	−0.06	0.61	0.90	0.60	0.68	**1**	−0.27	−0.27	0.64
	Sig.	0.00	0.00	0.00		0.98	0.79	0.00	0.00	0.00	0.00		0.12	0.12	0.00
NC	R	−0.22	0.29	0.35	−0.00	**1**	0.95	0.66	−0.16	0.43	0.46	−0.27	**1**	0.96	0.69
	Sig.	0.33	0.21	0.12	0.98		0.00	0.00	0.24	0.03	0.02	0.12		0.00	0.00
NF	R	−0.28	0.36	0.45	−0.06	0.95	**1**	0.55	−0.17	0.44	0.47	−0.27	0.96	**1**	0.67
	Sig.	0.21	0.11	0.04	0.79	0.00		0.01	0.23	0.03	0.02	0.12	0.00		0.00
NDVI	R	0.29	0.81	0.75	0.61	0.66	0.55	**1**	0.33	0.93	0.89	0.64	0.69	0.67	**1**
	Sig.	0.12	0.00	0.00	0.00	0.00	0.01		0.04	0.00	0.00	0.00	0.00	0.00	

Note: PH = plant height (cm), LL = leaf length (cm), LW = leaf width (cm), SD = stem diameter (mm), NC = number of clusters, NF = number of fruits, NDVI = Normalized Difference Vegetative Index, R = Pearson's correlation coefficient, and Sig = significance.

According to the correlation matrix, the agronomic variables show a moderate to high correlation with the variables of interest (yield and NDVI). The correlation coefficient indicates that, at least in the range of data analyzed, the assumption of multivariate linearity is reasonable and allows a more straightforward interpretation of the effects of each variable on the responses of interest. Likewise, using linear models implies coefficient βis that represent the direct marginal effect of each independent variable, avoiding overfitting and reducing complexity, which translates into a parsimonious approach. However, if subsequent studies detect that the relationship between the variables is not strictly linear, it

would be convenient to test other types of models (non-linear) or more flexible statistical models to determine whether the conclusions are still valid in these cases.

To use the Pearson correlation coefficient, one must first check whether there is a linear relationship between the independent and dependent variables. As noted by [58], there is evidence of a significant linear relationship between NDVI and yield (R^2 = 0.78), which supports the use of this coefficient in these cases. The Pearson coefficient is used precisely to verify this linear relationship, as seen when relating NDVI with PH, LL, LW, SD, NC, and NF, obtaining moderate to high correlation values (Table 4). However, when yield is considered an independent variable, the correlation with the covariates is more moderate, suggesting the need to evaluate whether this linear approach is the most appropriate in this case or whether another analysis method should be applied.

3.2. Regression Models

Linear multiple regression models with successive steps were obtained in groups of consecutive weeks, the vegetative stage between weeks 1 and 8, and the reproductive stage between weeks 9 and 28. Models were created to predict and project weekly yields per bed, using the statistically significant variables for each variety. These models are represented by variety as follows.

3.2.1. Beef Tomato

The model obtained for the beef variety has R^2 values of 0.982 between the first and eighth weeks (Figure 2). In contrast, for the following weeks (between 9 and 28) (Figure 3), the model yielded a coefficient of determination of 0.445, which indicates the complexity of predicting reproductive stage development based on the agronomic variables used. Generally, higher correlation values are observed when sensors are used in UAVs since they can cover larger areas and avoid these types of factors [21].

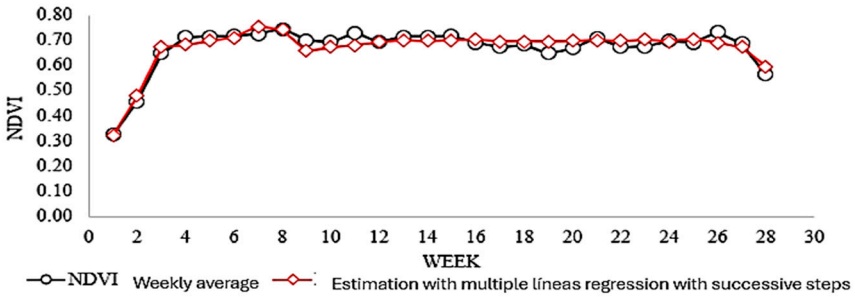

Figure 2. Average weekly NDVI for beef tomato and NDVI estimation with multiple regression.

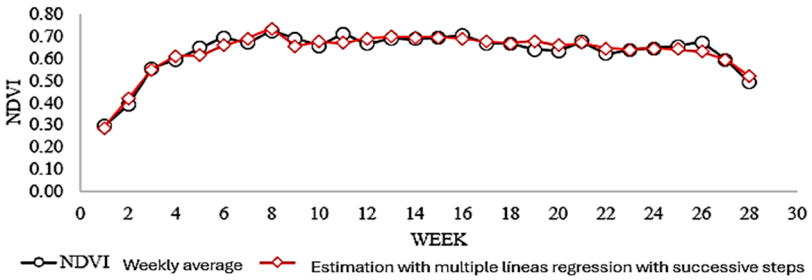

Figure 3. Average weekly NDVI for saladette tomato and NDVI estimation with multiple regression.

However, the coefficient of determination is relatively low at some stages of the model. For example, for beef tomatoes between weeks 9 and 28, the R^2 is 0.445, which indicates a limited predictive capacity. In addition, the article does not compare this model with other regression models to validate its suitability.

A value similar to that described by [59] was found using other, more complex models on aerial images of NDVI and agronomic variables to increase the coefficient, such as random forest, ridge regression, and support vector machines, 0.08 to 0.45, or the growth curves of the different organs of the tomato plant reported by [60] that were generated from growth analysis, finding three well-defined phases: an exponential one in the first four weeks after transplanting, a linear one from the fourth week, and a final decreasing trend when crop growth stopped, similar to the vegetative development found. The coefficients obtained for the equation corresponding to the beef tomato are shown in Table 5.

Table 5. Unstandardized coefficients between weeks for the variety of beef tomato.

Beef Tomato							
Weeks 1–8				**Weeks 9–28**			
Model	**Non-Standardized Coefficients**	**t**	**Sig.**	**Model**	**Non-Standardized Coefficients**	**t**	**Sig.**
	B				**B**		
(Constant)	0.086486	2.142	0.085	(Constant)	0.576650	19.296	0.000
Week	−0.025659	−2.609	0.048	NC	0.014973	3.797	0.001
SD	0.071309	8.632	0.000				
Independent variable: NDVI							

Note: Week = week number, SD = stem diameter (mm), NC = number of clusters, t = calculated t, and Sig = significance.

The statistical model obtained for the NDVI is presented in Equation (1) below:

$$\text{NDVI (weeks 1–8)} = 0.086486 + (-0.025659 \times \text{WEEK}) + (0.071309 \times \text{SD}) \quad (1)$$

where

- WEEK = number of weeks after transplanting;
- SD = stem diameter.

The statistical model obtained for the NDVI between weeks 9 and 28 based on the number of clusters is represented in the following equation:

$$\text{NDVI (weeks 9–28)} = 0.576650 + (0.014973 \times \text{NC}) \quad (2)$$

where

- NC = number of clusters.

The agronomic variable stem diameter had a statistically significant difference with the number of weeks in Equation 1. This corresponds to the vegetative stage between the first and eighth weeks, showing a high degree of correlation (R^2 = 0.982), which indicates a high predictive value of the model during the first stage of the crop. This phase was highlighted by the pronounced increase in the NDVI, which started with values of NDVI = 0.32, increasing to its maximum point in the eighth week with a value of NDVI = 0.74, according to values from the Green Seeker® sensor. The maximum NDVI value was in the seventh week, with a value of NDVI = 0.75, with only a difference of 0.01 index points.

From the ninth week after transplanting, the NR variable presented a statistically significant difference compared to the other variables due to its correlation with yield. However, the model presented a decrease in its coefficient of determination R^2= 0.445, as represented in Equation 2; this indicates the complexity of predicting plant development during the reproductive stage, according to the model created. However, the coincidence of the predictions of the generated model with the real values of NDVI obtained from Green Seeker® is observed (Figure 3).

3.2.2. Saladette Tomato

The models for the saladette variety had a coefficient of determination of 0.974 between the first and eighth weeks, also showing a great adjustment of the variable to the equation. The following model yielded a coefficient of determination of 0.764 between the ninth and twentieth weeks, showing an improvement with respect to the formula used in the same period of development in the beef tomato. The coefficients obtained for both equations corresponding to the beef tomato are presented in Table 6.

Table 6. Coefficients of determination for tomato variety saladette.

Saladette Tomato							
Model	**Non-Standardized Coefficients**	**t**	**Sig.**	**Model**	**Non-Standardized Coefficients**	**t**	**Sig.**
	B				**B**		
(Constant)	0.096468	2.933	0.026	(Constant)	0.315427	6.427	0.000
SD	0.056048	15.006	0.000	LL	0.004771	4.514	0.000
				NT	0.012435	3.386	0.004

Note: Dependent variable: NDVI; SD = stem diameter (mm), LL = leaf length, t = calculated t, and Sig = significance.

The statistical model obtained for the NDVI is presented in the following equation:

$$NDVI = 0.096468 + (0.056048 \times SD) \quad (3)$$

where

- SD = stem diameter.

Meanwhile, the statistical model obtained for the NDVI between weeks 9 and 28, based on leaf length and number of clusters, is represented by the following equation:

$$NDVI = 0.315427 + (0.004771 \times LL) + (0.012435 \times NC) \quad (4)$$

where

- LL = leaf length;
- NC = number of clusters.

Equation (3) presents a high coefficient of determination with $R^2 = 0.974$, demonstrating a great predictive capacity. In the case of the beef variety tomato, it can be observed that, starting from NDVI values of 0.29, it reaches a value with a maximum point of 0.72, as recorded by the Green Seeker® sensor and the predictive mathematical model, marking the end of this stage and the maximum point of vegetative development.

From week 9 onwards, the crop began to develop, reaching NDVI values ranging from 0.66 to 0.70, indicating that vegetative development of the plant was no longer a priority. The predictor equation generated at this stage obtained a coefficient of determination of $R^2 = 0.764$ using the NR variable, and unlike its equivalent in beef tomato, LH acted as a statistically significant variable. The curves generated based on the equations showed almost identical development to the model based on Green Seeker® sensor readings, demonstrating that the sensor could be used for development prediction in subsequent cycles. Multiple regression models were used to predict the yield of the two tomato varieties (beef and saladette tomato) using NDVI and the measured agronomic variables; only the variables that showed statistical significance were included in the equations.

With respect to the beef tomato, a statistically significant model was obtained ($p = 0.95$) at a level of $\alpha = 0.05$ and a coefficient of $R^2 = 0.397$, which indicates a 39.7% explanation of the variation in Y given by the values of X, with the remaining 61% of the variation in

production given by other factors. The variables that are not included in this model are not necessarily inefficient for the calculation; however, they do not provide more information for the estimation, so they are discarded.

The model obtained for the performance prediction was as follows:

$$Yield = 40.810 + (0.144 \times PH) + (-1.663 \times LL) + (1.842 \times NF) \quad (5)$$

where

- PH = plant height;
- LL = Leaf length;
- NF = number of fruits.

3.2.3. Saladette Tomato Yield

The saladette tomato generated a statistically significant relationship ($p = 0.95$) at a level of $\alpha = 0.05$ and a coefficient of $R^2 = 0.265$, indicating a 26.5% explanation of the variation in Y given by the values of X, with the remaining 73.5% of the variation in production given by other factors not included in the model, as was the case with the previous model.

The model obtained for performance prediction was as follows:

$$Yield = -130.8 + (0.249 \times PH) + (1.478 \times LW) \quad (6)$$

where

- PH = plant height;
- LW = leaf width.

The accuracy of the model is low compared to other models [61] when using similar variables (number of fruits) with accuracies ranging from 0.7 to 0.8; however, the results show possible outliers and a very high variance, which agrees with the values of the metrics for Equations (5) and (6). Likewise, the models based on the NDVI obtain results with low correlations (0.44) for yield (kg/plant) [62], with both equations discarding the NDVI due to the low explanation of the variance of the yield (Table 7).

Table 7. Performance model accuracy metrics.

Variety	MAE	MSE	RMSE	R^2
Beef	21.2	817	28.6	0.397
Saladette	15.8	462	21.5	0.265

3.3. Thematic NDVI and Yield Maps

The thematic maps generated by the simple Kriging model through the exploratory analysis of data distribution indicate a normal distribution of the information captured by the sensor and agronomic variables, corroborating the choice of Kriging as a method for point data interpolation since it minimizes the error variance, using a weighted linear combination of the data similar to that reported by [63]. This is due to the large number of sampling points captured and the spatial distribution of them within the greenhouse, and the model minimized the variance error.

The maps generated show how the vegetation index increases as the weeks go by, reaching its peak in week 8 (Figure 4). The Green Seeker® sensor has been considered a promising tool for predicting yield in various crops, especially in grain crops such as wheat [33]. It also obtained a high level of correlation with the significant variables for each model during the first weeks of the tomato crop. Therefore, its use allows

for predicting vegetative development and assessing nutritional status in real time, as proposed by [64]. As [65] points out, the Green Seeker sensor is very useful for estimating biomass during the vegetative stage of crops, which explains its effectiveness in modeling that phase. Nevertheless, in this study, the model developed for calculating yield in both varieties does not include NDVI as a statistically significant variable, indicating that it does not have much relevance in the equation for estimating the yield of indeterminate-type tomatoes. This difference in results is likely because most of the studies for yield calculation have been carried out on determinate crops, whose productive cycle does not extend for months. The authors of [66] mentioned that the sensor can monitor crop growth, correlate with production traits of the barley plant, and predict yield; however, due to the low significance of NDVI within the statistical model generated with the variables studied for yield calculation, it was not possible to obtain this prediction in tomato. The multiple regression model allowed the modeling of the development curve using the agronomic variables and NDVI. These NDVI time series are helpful for producers since they allow them to observe crop development, taking into account some variables related to soil properties, such as maximum rooting depth, water content at field capacity, and permanent wilting point of the soil, as mentioned by [67] when proposing a methodology to predict time series using data from previous cycles in soybean cultivation.

This methodology can significantly improve the model generated for tomato yield prediction by including these variables in future agricultural cycles. However, some drawbacks of the sensor are the NDVI readings that vary according to the angle and height of the instrument during its use [41], becoming a disadvantage, which is paramount to standardizing a protocol for the use of the sensor that decreases these variations in the measurement [68]. Therefore, there is a zenith angle perpendicular to the canopy (90 degrees) between the emission and reception of the sensor in the sweep of the cultivars section, regardless of the solar declination or tilt angle regarding the time of day. This is due to the ease of erroneously recording mean values of continuous sections and modifying the NDVI point readings and, thus, thematic maps within the greenhouse.

The results of the present research can be compared with previous agronomic research since sensors for agriculture have accelerated the digitization of farms in intensive production systems, as reported by [69], who, according to a previous calibration and validation of the optical sensor, after obtaining a yield prediction equation, substantially reduced production costs. Consequently, data analysis was fundamental in evaluating crop health status and planning specific nitrogen fertilization actions at the commercial level in development stages employing mathematical diagnostic models [70]. However, in indeterminate crops, this variable no longer reflects the benefits in yield projection due to the very nature of the tomato crop, which continues to develop its canopy indeterminately with similar index values without obtaining those proportional to the yield, as was presented in the first weeks of production. As reported by [71], changes in vegetation, monitored through NDVI, can influence agricultural productivity. This fact aligns with our observations that NDVI is an excellent indicator of vegetative progress but not necessarily of final yield under protected agriculture conditions.

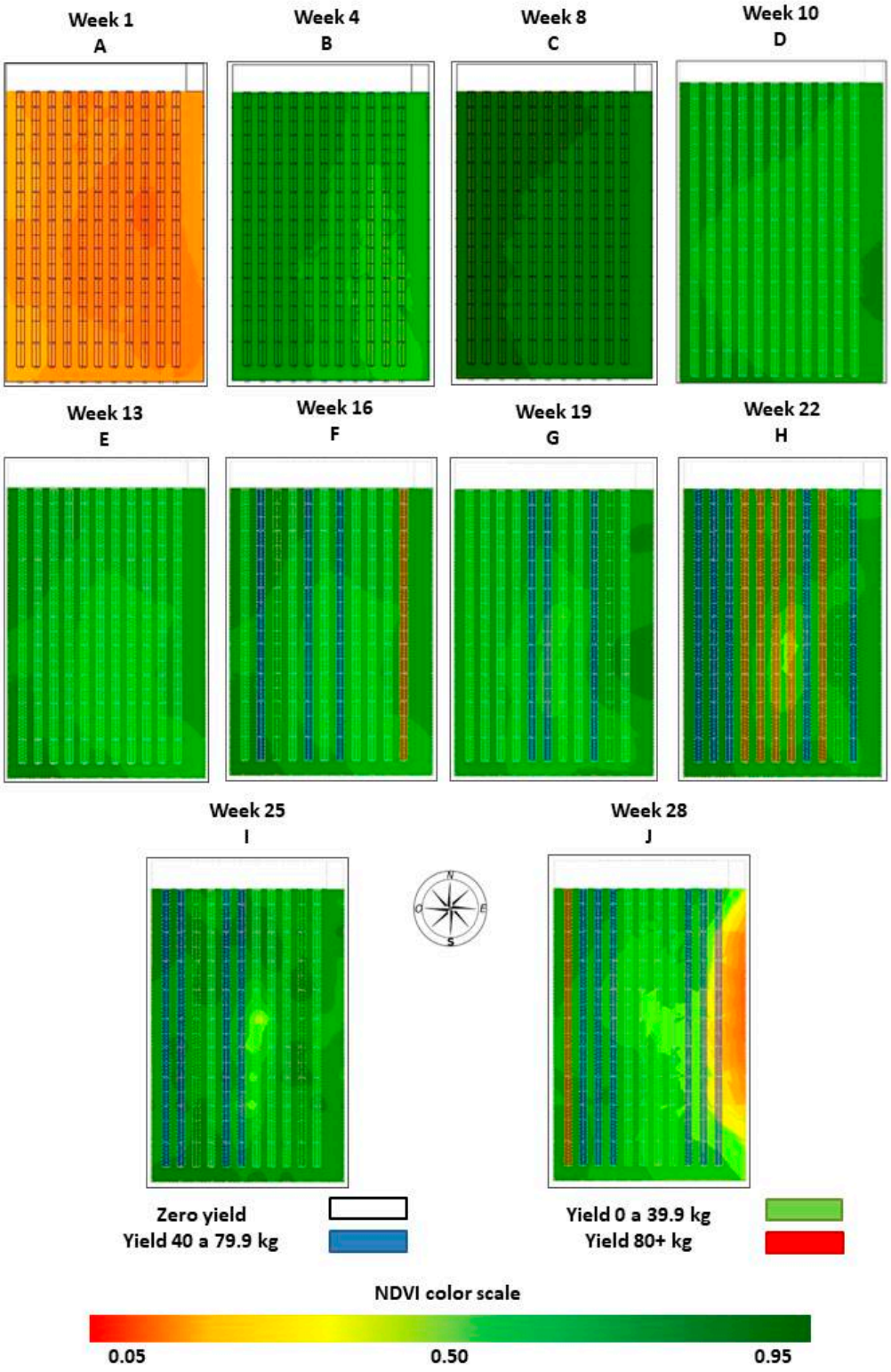

Figure 4. NDVI distribution map in different weeks and yield ranking by bed: (**A**) week 1; (**B**) week 4; (**C**) week 8; (**D**) week 10; (**E**) week 13; (**F**) week 16; (**G**) week 19; (**H**) week 22; (**I**) week 25; and (**J**) week 28.

If a variety is selected in the production system, how the environment influences the efficient use of resources will be seen. At the end of the cycle, yield is the static and final result of a crop's behavior. As mentioned by [72], this event does not reflect the interactions existing during the cycle between agronomic management and the production environment, which makes it challenging to evaluate the relationships existing during the

cycle between agronomic management and the production environment, resulting in a decrease in yield, as observed in our research, which from week 18 onwards declined to become economically unprofitable.

NDVI maps are crucial tools for examining tomato crop conditions, as they allow for visualization of the spatial distribution of vegetation and detection of problem areas related to leaf cover, foliage density, and disease presence, factors that directly influence vegetation indices [73]. Likewise, using NDVI and other indices is fundamental to evaluating yield and agronomic variables of tomatoes through spectroradiometry and Ordinary Kriging, which contributes to detecting areas with water stress and its influence on fruit productivity [74]. On the other hand, [75] points out that NDVI is fundamental to examining the spatial and temporal variability of industrial tomato yield, evidencing a high correlation between the index and productivity in both terrestrial and orbital measurements, thus reinforcing the ability to use NDVI maps at various scales and consolidating its relevance in precision agriculture. Ultimately, the use of spatiotemporal data in maps makes it possible to identify the spatial variability of the crop under various conditions, and by combining vegetation spectral indices with agronomic variables, its growth over time can be evaluated, contributing to the management and planning of the productive system, the planning of activities such as irrigation scheduling, or constant monitoring of phenology and crop development [76,77].

Plant height showed high variance during the first week, indicating more significant initial heterogeneity. Throughout the weeks, height values remained in medium to high ranges, which reached their most extraordinary heterogeneity until week 28. About the length and width of leaves, a decrease in the behavior of the beef tomato variety compared to the saladette was observed. However, during the ninth week, values increased in both varieties, showing a greater length and width in beef compared to saladette, the latter being the one with the most excellent vegetative development recorded during week 28. However, the diameters of the two varieties do not reflect a dominant trend because similar values were recorded between both varieties, except in the previous week for the saladette variety (Figure 5 and Table 8) (with a reduced size).

Table 8. Minimum, medium, and maximum values of the agronomic variables.

Variables/Week	Low			Medium			High		
	1	**9**	**28**	**1**	**9**	**28**	**1**	**9**	**28**
Height	17	58	283	22	159	532	24	214	532
Length leaf	4	45	31	15	52	38	21	57	41
Width leaf	1	33	32	11	49	39	14	58	41
Stem	2.5	10	14.5	3	11.5	15.7	3.5	12.2	15.9
Number of bunches	5	7	0	6	9	1	6	9	4
Number of fruits	9	21	1	12	21	1	13	29	2

Note: Average point values of the lines of each section of the beds.

Regarding the number of bunches and fruit per plant, the beef variety experienced a reduction during the week, while the saladette experienced more bunches and fruit during the same period (Figure 6 and Table 8).

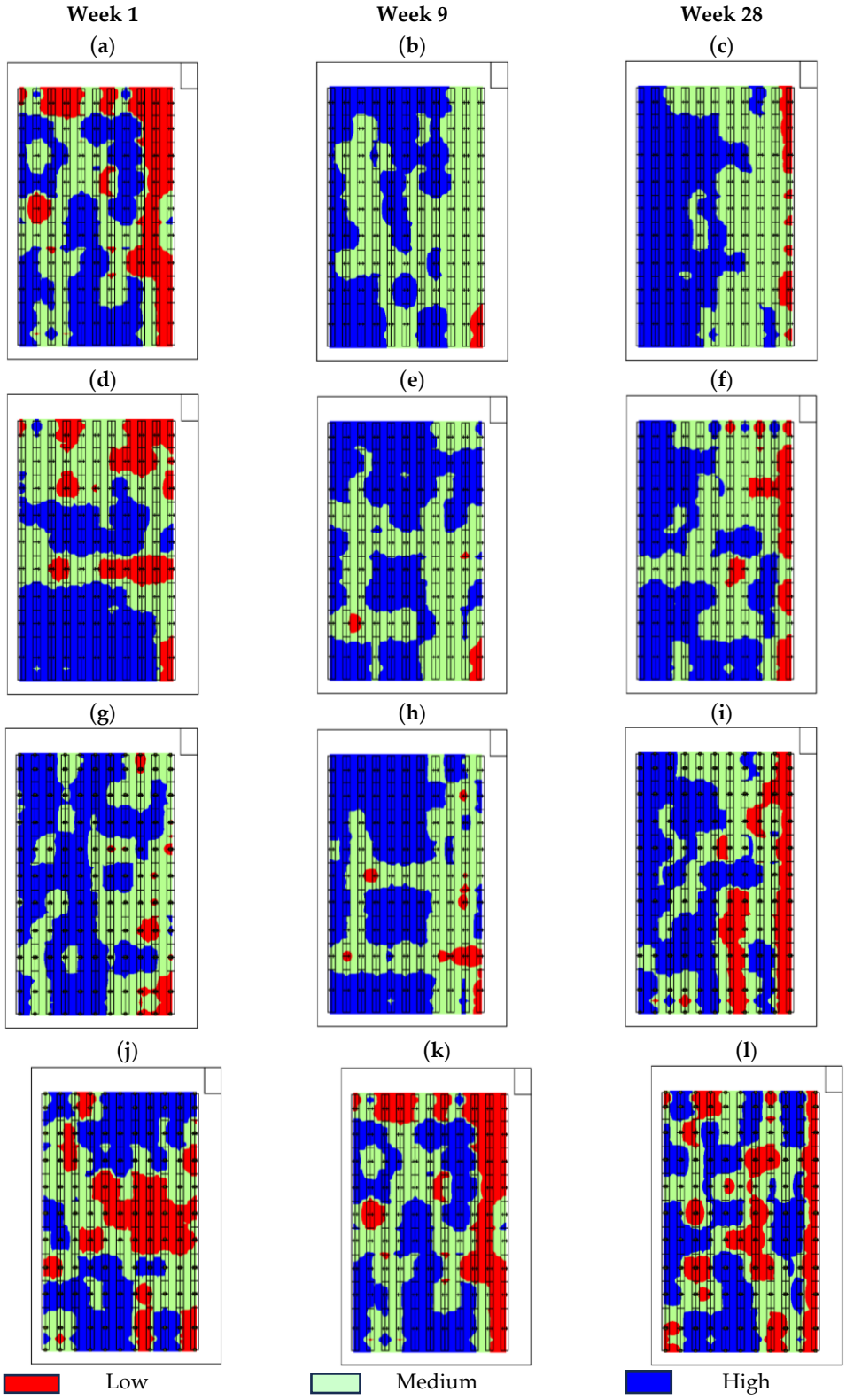

Figure 5. Thematic maps of (**a**–**c**) height; (**d**–**f**) length leaf; (**g**–**i**) width leaf; (**j**–**l**) stem.

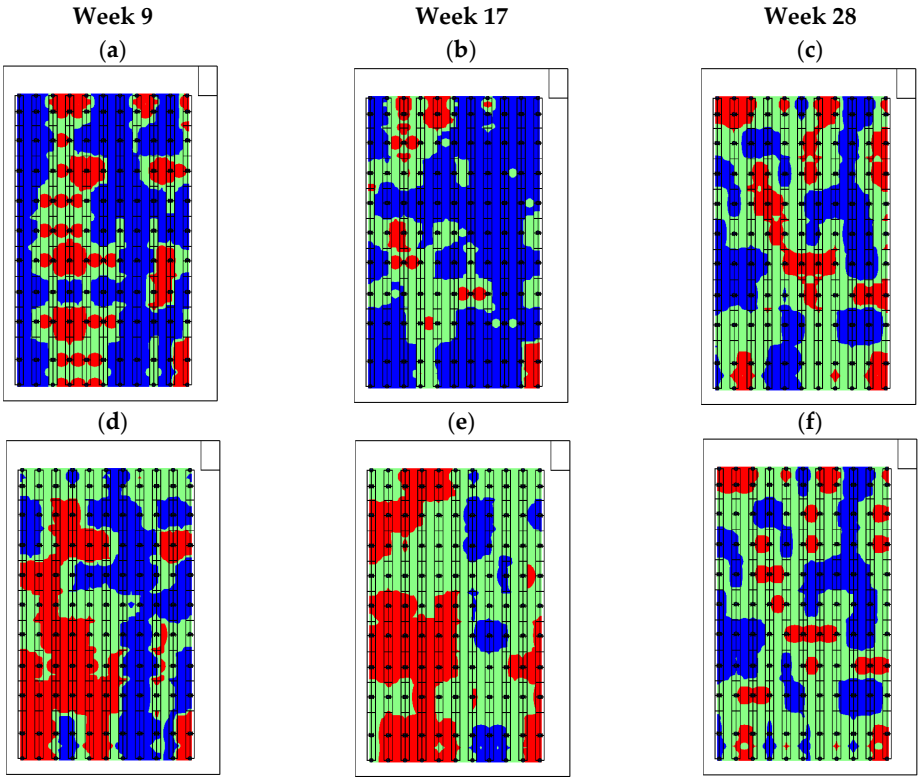

Figure 6. Thematic maps of (**a**–**c**) number of bunches; (**d**–**f**) number of fruits.

4. Conclusions

NDVI-based models were unreliable for predicting the yield of indeterminate tomatoes in protected agriculture systems due to a drop in yield at later stages of production. Other variables that can improve the accuracy of predictive models should be examined, and additional sensors should be adopted for a more complete monitoring of leaf development with a certainty of higher yield.

The Green Seeker® NDVI field sensor is a useful tool that provides accurate information on the absence or absence of chlorosis in plant leaves caused by a nutrient deficiency. However, it is necessary to consider the costs of investment and support personnel for its interpretation, as well as the fact that the Green Seeker® field sensor has limitations that can affect its reading, such as the angle of the sensor in relation to the plants during sample collection. Since its area of action is conical, any change in position could result in a different interpretation in terms of the continuous vegetation of the target. It is important to monitor by sections or zones within the greenhouse, not as a single unit.

The equations and statistical models evaluated only apply to cultivating tomatoes of indeterminate variety under protected agriculture and intensive production system conditions, which should be contrasted with agronomic variables in each agricultural cycle.

Author Contributions: Conceptualization, E.V.G.-C. and J.A.S.-N.; methodology, E.V.G.-C.; software, G.A.R.-G.; formal analysis, G.A.R.-G. and E.O.-S.; investigation, E.V.G.-C. and J.A.S.-N.; resources, E.V.G.-C.; writing—original draft preparation, E.V.G.-C. and J.A.S.-N.; writing—review and editing, F.D.G.-M. and V.V.E.-U. All authors have read and agreed to the published version of the manuscript.

Funding: This research was found by Universidad Autónoma de Nuevo León (UANL).

Data Availability Statement: The original contributions presented in this study are included in the Supplementary Material. Further inquiries can be directed to the corresponding author.

Acknowledgments: The authors would like to thank the Universidad Autónoma de Nuevo León (UANL) for providing the research area.

Conflicts of Interest: The authors declare no conflicts of interest. The funders had no role in the design of the study, in the collection, analyses, or interpretation of data, in the writing of the manuscript, or in the decision to publish the results.

References

1. La Cecilia, D.; Tom, M.; Stamm, C.; Odermatt, D. Pixel-basel mapping of open field and protected agricultures using constrained Sentinel-2 data. *ISPR Open J. Photogramm. Remote Sens.* **2023**, *8*, 100033. [CrossRef]
2. Villagran, E.A.; Eliecer Jaramillo, J.; León Pacheco, J.; Ramírez Matarrita, R. Diurnal microclimatic behavior, during the dry season, of three structures for protected agriculture in the dry tropics. *UNED Res. J.* **2020**, *12*, e2854. [CrossRef]
3. McCartney, L.; Lefsryd, M.G. Protected agriculture in extreme environments: A review of controlled environment agriculture in tropical, arid, polar, and urban locations. *Apppl. Eng. Agric. Am. Soc. Agric. Biol. Eng.* **2018**, *32*, 455–473. [CrossRef]
4. Flores, J.; Ojeda Bustamante, W.; López, I.; Rojano, A.; Salazar, I. Requerimientos de riego para tomate de invernadero. *Terra Latinoaméricana* **2007**, *25*, 127–134.
5. Ntinas, G.K.; Neumair, M.; Tsadilasb CMeyer, J. Carbon footprint and cumulative energy demand of greenhouse and open-field tomato cultivation systems under southern and central European climatic conditions. *J. Clean. Prod.* **2017**, *142*, 3617–3626. [CrossRef]
6. Xue, J.; Su, B. Significant remote sensing vegetation indices: A review of developments and applications. *J. Sens.* **2017**, *2017*, 1353691. [CrossRef]
7. Taylor, S.N.; Hegarty, J.; Tamagno, S.; Lundy, M.E. NDVI-based ideotypes as a cost-Effective tool to support wheat yield stability selection under heterogeneous environments. *Field Crops Res.* **2025**, *322*, 109727. [CrossRef]
8. Canaj, K.; Morrone, D.; Roma, R.; Boari, F.; Cantore, V.; Todorovic, M. Reclaimed water for vineyard irrigation in a Mediterranean context: Life cycle environmental impacts, life cycle costs, and eco-efficiency. *Water* **2021**, *13*, 2242. [CrossRef]
9. D'Amico, A.; De Boni, A.; Palmisano, G.O.; Acciani, C.; Roma, R. Environmental analysis of soilless tomato production in a high-tech greenhouse. *Clean. Environ. Syst.* **2023**, *11*, 100137. [CrossRef]
10. Fullana Pericas, M.; Conesa, M.A.; Gago, J.; Ribas Carbó, M.; Galmés, J. High-throughput phenotyping of a large tomato collection underwater deficit: Combining UAV's remote sensing with conventional leaf-level physiologic and agronomic measurements. *Agric. Water Manag.* **2022**, *260*, 107283. [CrossRef]
11. Forest, R.; Prieto, M.H.; Garcia Martín, A.; Córdoba, A.A.; Martínez, L.; Campillo, C. Using NDVI and guided sampling to develop yield prediction maps of processing tomato crops. *Span. J. Agric. Res.* **2015**, *13*, e0204. [CrossRef]
12. Moscovini, L.; Ortenzi, L.; Pallottino, F.; Figorilli, S.; Violino, S.; Pane, C.; Capparella, V.; Vasta, S.; Costa, C. An open-source machine-learning application for predicting pixel-to-pixel NDVI regression from RGB-calibrated images. *Comput. Electron. Agric.* **2024**, *216*, 108536. [CrossRef]
13. Vikuk, V.; Spirkaneder, A.; Noack, P.; Dueming, A. Validation of a sensor-system for real-time measurement of mineralized nitrogen in soils. *Smart Agric. Technol.* **2024**, *7*, 100390. [CrossRef]
14. Maselli, F.; Battista, P.-; Chiesi, M.; Rapi, B.; Angeli, L.; Fibbi, L.; Magno, R.; Gozzini, B. Use of sentinel-2 MSI data to monitor crop irrigation in Mediterranean area. *Int. J. Appl. Earth Obs. Geoinf.* **2020**, *93*, 102216. [CrossRef]
15. Eklundth, L.; Jönsson, P. *Timesat 3.0 Software Manual*; Lund University: Lund, Sweden, 2009.
16. Paruelo, J.M.; Jobbágy, E.G.; Sala, O.E. Current distribution of ecosystem functional 593 types in temperate South America. *Ecosystems* **2001**, *4*, 683–698. [CrossRef]
17. Carlson, T.N.; Arthur, S.T. The impact of land use—Land cover changes due to urbanization on surface microclimate and hydrology: A satélite perspective. *Glob. Planet. Change* **2000**, *25*, 49–65. [CrossRef]
18. Sajitha, P.; Andrushia, A.D.; Anand, N.; Naser, M.Z. A review on machine learning and deep learning image-based plant disease classification for industrial farming systems. *J. Ind. Inf. Integr.* **2024**, *38*, 100572. [CrossRef]
19. Li, D.; Li, C.; Yao, Y.; Li, M.; Liu, L. Modern imaging techniques in plant nutrition analysis: A review. *Comput. Electron. Agric.* **2020**, *174*, 105459. [CrossRef]
20. Mateo Sanchez, A.; Piles, M.; Muñiz Mari, J.; Adusuara, J.E.; Pérez Suay, A. Synergistic integration of optical and microwave satellite data for crop yield estimation. *Remote Sens. Environ.* **2019**, *234*, 111460. [CrossRef]
21. Enciso, J.; Avila, C.A.; Jung, J.; Elsayed Farag, S.; Anjin, C.; Yeom, J.; Landivar, J.; Maeda, M.; Chavez, J.C. Validation of agronomic UAV and field measurements for tomato varieties. *Comput. Electron. Agric.* **2019**, *158*, 279–283. [CrossRef]
22. Vinces Llaguno, L.S.; Trujillo Reyes, Y. Modelo de comportamiento de las temperaturas medias en el cultivo de tomate (*Solanum licopersicum*). *Reevista Cuba. De Meteorol.* **2021**, *27*, 1–5.
23. Nolasco, M.; Martínez, M.; Bocco, M. Trigo en la provincia de Córdoba: ¿Cómo identificarlo y caracterizar su ciclo usando solamente series temporales de NDVI. *Nexo Agropecu.* **2024**, *12*, 7–150. Available online: https://revistas.unc.edu.ar/index.php/nexoagro/article/download/44541/45871/187261 (accessed on 20 December 2024).

24. Huang, J.; Wang, H.M.; Dai, Q.; Han, D. Analysis of NDVI data for crop identification and yield estimation. *IEEE J. Sel. Top. Appl. Earth Obs. Remote Sens.* **2014**, *7*, 4374–4384. [CrossRef]
25. Miller, J.O.; Mondal, P.; Sarupria, M. Sensor-based measurements of NDVI in small grain and corn fields by tractor, drone, and satellite platforms. *Crop Environ.* **2024**, *3*, 33–42. [CrossRef]
26. Pérez, J.L. Impacto de las tecnologías disruptivas en la percepción remota: Big data, 596, internet de las cosas e inteligencia artificial. *UD Y La Geomática* **2019**, *14*, 54–61.
27. Zhang, K.; Liu, X.; Ma, Y.; Wang, Y.; Cao, Q.; Zhu, Y.; Tian, Y. A new canopy chlorophyll index-based paddy rice critical nitrogen dilution curve in eastern China. *Field Crops Res.* **2021**, *266*, 108–139. [CrossRef]
28. Rambo, L.; Ma, B.L.; Xiong, Y.; Regis Ferreira da Silvia, P. Leaf and canopy optical characteristics as crop-N-status indicators for field nitrogen management in corn. *J. Plant Nutr. Soil Sci.* **2010**, *173*, 434–443. [CrossRef]
29. Katsoulas, N.; Elvanidi, A.; Ferentinos, K.P.; Kacira, M.; Bartzanas, T.; Kittas, C. Crop reflectance monitoring as a tool for water stress detection in greenhouses: A review. *Biosyst. Eng.* **2016**, *151*, 374–398. [CrossRef]
30. Neiff, N.; Dhliwayo, T.; Suarez, E.A.; Burgueno, J.; Trachsel, S. Using an airborne platform to measure canopy temperature and NDVI under heat stress in maize. *J. Crop Improv.* **2015**, *29*, 669–690. [CrossRef]
31. Barros, A.S.; Farias, L.M.; Marinho, J.L.A. Aplicação do Índice de Vegetação por 456 Diferença Normalizada (NDVI) na Caracterização da Cobertura 2020 Vegetativa de Juazeiro Do 457 Norte–CE. *Rev. Bras. De Geogr. Física* **2020**, *13*, 164–172. [CrossRef]
32. Aparicio, N.; Villegas, D.; Royo, C.; Casadesus, J.; Araus, J.L. Effect of sensor view angle on the assessment of agronomic traits by ground level hyper-spectral reflectance measurements in durum wheat under contrasting Mediterranean conditions. *Int. J. Remote Sens.* **2004**, *25*, 1131–1152. [CrossRef]
33. Ali, A.M.; Ibrahim, S.M. Wheat grain yield and nitrogen uptake prediction using at Leaf and GreenSeeker portable optical sensors at jointing growth stage. *Inf. Process Agric.* **2020**, *7*, 375–383. [CrossRef]
34. Grados, D.; Reynarfaje, X.; Schrevens, E. A methodological approach to assess canopy 5 NDVI–based tomato dynamics under irrigation treatments. *Agric. Water Manag.* **2020**, *240*, 106208. [CrossRef]
35. Enciso, J.; Maeda, M.; Landivar, J.; Jung, J.; Chang, A. A ground based platform for high throughput phenotyping. *Comput. Electron. Agric.* **2017**, *141*, 286–291. [CrossRef]
36. Campos, J.; García Ruiz, F.; Gil, E. Assessment of vineyard canopy characteristics from vigour maps obtained using UAV and satellite imagery. *Sensors* **2021**, *21*, 2363. [CrossRef]
37. Ruan, G.; Li, X.; Yuan, F.; Cammarani, D. Improving wheat yield prediction integrating proximal sensing and weather data with machine learning. *Comput. Electron. Agric.* **2022**, *195*, 106852. [CrossRef]
38. Jiang, J.; Zhang, Z.; Cae, Q.; Liang, Y.; Krienke, B.; Tian, Y.; Zhu, Y.; Cae, W.; Liu, X. Use of an active canopy sensor mounted on an unmanned aerial vehicle to monitor the growth and nitrogen status of winter wheat. *Remote Sens.* **2020**, *12*, 3684. [CrossRef]
39. Muñoz Huerta, R.F.; Guevara Gonzalez, R.G.; Contreras Medina, L.M.; Torres Pacheco, I.; Prdado Olivarez, J.; Ocampo Velazquez, R.V. A Review of methods for sensing nitrogen status in plants: Advantages, disadvantages and recent advances. *Sensors* **2013**, *13*, 10823–10843. [CrossRef] [PubMed]
40. Padilla, F.M.; Gallardo MPeña Fleitas, M.T.; de Souza, R.; Thompson, R.B. Proximal optical sensors for nitrogen management of vegetable crops: A review. *Sensors* **2018**, *18*, 2083. [CrossRef] [PubMed]
41. Kim, Y.; Glenn, D.M.; Park, J.; Ngugi, H.K.; Lehman, B.L. Characteristics of active spectral sensors for plant sensing. *Trans. ASABE* **2012**, *55*, 293–301. [CrossRef]
42. Kipp, S.; Mistele, B.; Schmidhalter, U. The performance of active spectral reflectance sensors is influenced by measuring distance, device temperature, and light intensity. *Comput. Electron. Agric.* **2014**, *100*, 24–33. [CrossRef]
43. Gnyp, M.L.; Miao, Y.; Yuan, F.; Ustin, S.L.; Yu, K.; Yao, Y.; Huang, S.; Bareth, G. Hyperspectral canopy sensing of paddy rice aboveground biomass at different growth stages. *Field Crops Res.* **2014**, *155*, 42–55. [CrossRef]
44. Van Loon, J.; Speratti, A.B.; Gabarra, L.; Govaerts, B. Precision for smallholders farmers: A small-scale-tailored variable rate fertilizer application kit. *Agriculture* **2018**, *8*, 48. [CrossRef]
45. Barker, J., III; Zhang, N.; Sharon, J.; Steeves, R.; Wang, X.; Wei, Y.; Poland, J. Development of a field-based high-throughput mobile phenotyping platform. *Comput. Electron. Agric.* **2016**, *122*, 74–85. [CrossRef]
46. Servicio de Información Agroalimentaria y Pesquera (SIAP), Anuario Estadístico de la Producción Agrícola. Available online: https://nube.siap.gob.mx/cierreagricola (accessed on 18 January 2025).
47. Singh, R.K.; Rahmani, M.H.; Weyn, M.; Berkvens, R. Join communication and sensing: A proof of concept and dataset for greenhouse monitoring using LoRaWAN. *Sensors* **2022**, *22*, 1326. [CrossRef] [PubMed]
48. Gong, X.; Bo, G.; Liu, H.; Ge, J.; Li, X.; Gao, S. Performance of the Improved Pristley-Taylor model for simulating evapotranspiration of greenhouse tomatoes at different growth stages. *Planta* **2022**, *11*, 2956. [CrossRef]
49. Hamdane, Y.; Gracia Romero, A.; Buchaillot, M.L.; Sánchez Bragado, R.; Fullana, A.M.; Sorribas, F.J.; Araus, J.L.; Kefaucer, S.C. Comparison of proximal remote sensing devices of vegetable crops to determine the role of grafting in plant resistance to Meloidogyne incognita. *Agronomy* **2022**, *11*, 1098. [CrossRef]

50. Colimba Limaico, J.E.; Zubelzu Minguez, S.; Rodríguez Sinobas, L. Optimal irritgation scheduling for greenhouse tomato crop (*Solanum lucopersicum* L.) in Ecuador. *Agronomy* **2022**, *12*, 1020. [CrossRef]
51. Nikolaou, G.; Neocleous, D.; Christou, A.; Polycarpou, P.; Kitta, E.; Katsoulas, N. Energy and water-related parameters in tomato and cucumber greenhouse crops in semiarid Mediterranean regions. A review, part II: Irrigation and fertigation. *Horticulturae* **2021**, *7*, 548. [CrossRef]
52. Rezvani, S.M.-E.; Abyyaneh, H.Z.; Shamshiri, R.R.; Balasundram, S.K.; Dworak, V.; Goodarzi, M.; Sultan, M.; Mahns, B. IoT-Based sensor data fusion for determining optimality degrees of microclimate parameters in commercial greenhouse production of tomato. *Sensors* **2020**, *20*, 6474. [CrossRef] [PubMed]
53. Shi, K.; Ding, X.T.; Dong, D.K.; Zhou, Y.H. Root restriction-induced limitation to photosynthesis in tomato (*Lycopersicon esculentum Mill*) leaves. *Sci. Hortic.* **2008**, *117*, 197–202. [CrossRef]
54. Ara, N.; Bashar, M.K.; Begum, S.; Kakon, S.S. Effect of spacing and stem pruning on the 451 growth and yield of tomato. *Int. J. Sustain. Crop Prod.* **2007**, *2*, 35–39.
55. Mngoma, M.F.; Magwaza, L.S.; Sithole, N.J.; Magwaza, S.T.; Mditshwa, A.; Tesfay, S.Z.; Ncama, K. Effects of stem training on the physiology, growth, and yield responses of indeterminate tomato (*Solanum lycopersicum*) plants grown in protected cultivation. *Heliyon* **2022**, *8*, e09343. [CrossRef] [PubMed]
56. Dimokas, G.; Tchamitchian, M.; Kittas, C. Calibration and validation of a biological model to simulate the development and production of tomatoes in Mediterranean greenhouses during winter period. *Biosyst. Eng.* **2009**, *103*, 217–227. [CrossRef]
57. Trimble Navigation Limited®. *Operation Manual GreenSeeker Handheld Crop Sensor. Quick Reference Card*; Trimble Navigation Limited: Folsom, CA, USA, 2013.
58. Padilla, F.M.; Peña Fleita, M.T.; Gallardo, N.; Thompson, R.B. Threshold values of canopy reflectance índices and chlorophyll meter readings for optimal nitrogen nutrition of tomato. *Ann. Appl. Biol.* **2015**, *166*, 271–285. [CrossRef]
59. Tatsumi Morita YHeuvelink, E.; Khaleghi, S.; Bustos Korts, D.; Marcelis, L.F.M.; Vermeer, K.M.C.A.; Van Dijk, H.; Millenaar, F.F.; Van Voorn, G.A.K.; Van Eeuwijk, F.A. Yield dissection models to improve yield: A case study in tomato. *Silicio Plants* **2021**, *3*, diab012. [CrossRef]
60. Juarez Maldonado, A.; De Alba Romenus, K.; Zermeño González, A.; Ramírez, H.; Benavides Mendoza, A. Análisis de crecimiento del cultivo de tomate en invernadero. *Rev. Mex. De Cienc. Agrícolas* **2015**, *6*, 943–954. [CrossRef]
61. Tatsumi, K.; Igarashi, N.; Mengxue, X. Prediction of plant-level tomato biomass and yield using machine learning with unmanned aerial vehicle imagery. *Plants Methods* **2021**, *17*, 77. [CrossRef] [PubMed]
62. Ihuoma, S.O.; Madramootoo, C.A. Sensitivity of spectral vegetation indices for monitoring water stress in tomato plants. *Comput. Electron. Agric.* **2019**, *163*, 104860. [CrossRef]
63. Panagopoulos, T.; Jesús, J.; Blumberg, D.; Ben-Asher, J. Spatial variability of durum wheat yield as related to soil parameters in an organic field. *Comm. Soil Sci. Plant Anal.* **2014**, *45*, 2018–2031. [CrossRef]
64. Raun, W.R.; Solie, J.B.; Johnson, G.V.; Stone, M.L.; Lukina, E.V.; Thomason, W.E.; Schepers, J.S. In-season prediction of potential grain yield in winter wheat using canopy reflectance. *Agron. J.* **2001**, *93*, 131–138. [CrossRef]
65. Hassan, M.A.; Yang, M.; Rasheed, A.; Yang, G.; Reynolds, M.; Xia, X.; Xiao, Y.; He, Z. A rapid monitoring of NDVI across the wheat growth cycle for grain yield prediction using a multi-spectral UAV platform. *Plant Sci.* **2019**, *282*, 95–103. [CrossRef]
66. Fabbri, C.; Napoli, M.; Verdi, L.; Mancini, M.; Orlandini, S.; Dalla Marta, A. A Sustainability Assessment of the Greenseeker N Management Tool: A Lysimetric Experiment on Barley. *Sustainability* **2020**, *12*, 7303. [CrossRef]
67. Berger, A.; Ettlin, G.; Quincke, C.; Rodríguez-Bocca, P. Predicting the Normalized Difference Vegetation Index (NDVI) by training a crop growth model with historical data. *Comput. Electron. Agric.* **2019**, *161*, 305–311. [CrossRef]
68. Nogueira Martins, R.; Marcus Fialho e Moraes, H.; Fagundes Portes, M.; Orlando, W.D.A., Jr.; Furtado Ribeiro, M., Jr. Do optical sensor readings change throughout the day? An evaluation of two sensor systems. *J. Plant Nutr.* **2020**, *43*, 1689–1696. [CrossRef]
69. Santillano-Cázares, J.; López-López, A.; Ortiz-Monasterio, I.; Raun, W.R. Uso de sensores ópticos para la fertilización de trigo (*Triticum aestivum* L.). *Terra Latinoam. Chapingo* **2013**, *31*, 95–103.
70. Gutiérrez-Soto, M.V.; Cadet-Piedra, E.; Rodríguez-Montero, W.; Araya-Alfaro, J.M. El Green Seeker™ y el diagnóstico del estado de salud de los cultivos. *Agron. Mesoam.* **2011**, *22*, 397–403. Available online: http://www.scielo.sa.cr/scielo.php (accessed on 18 January 2025). [CrossRef]
71. Olivares, B.; López-Beltran, M. Normalized Difference Vegetation Index (NDVI) applied to the agricultural Indigenous territory of Kashaama, Venezuela. *UNED Res. J.* **2019**, *11*, 112–121. [CrossRef]
72. Verhulst, N.; Govaerts, B.; Fuentes Ponce, M. Sensor Portátil Green Seeker TM Para la Medición del índice Diferencial de Vegetación Normalizado (NDVI): Una Herramienta para la Evaluación Integral de las Prácticas Agronómicas. Parte A: Conceptos y Estudios de Caso. México, D.F.; CIMMYT. 2010. Available online: http://hdl.handle.net/10883/560 (accessed on 18 January 2025).
73. Candiago, S.; Remondigo, F.; De Giglio, M.; Gattelli, N. Evaluating multispectral images and vegetation indices for precision farming applications from UAV images. *Remote Sens.* **2015**, *7*, 4026–4047. [CrossRef]

74. Marino, S.; Cocozza, C.; Tognetti, R.; Alvino, A. Use of proximal sensing and vegetation indexes to detect the inefficient spatial allocation of drip irrigation In a spot area of tomato field crop. *Precis. Agric.* **2015**, *16*, 613–629. [CrossRef]
75. Martins, M.P.D.O.; Dos Reis, E.F.; Lopes, L.D.L. Spatial and temporal variability of vegetation indices with industrial Tomato Yield. *J. Sustain. Dev.* **2023**, *16*, 1–42. [CrossRef]
76. De Castro, A.I.; Six, J.; Plant, J.S.; Peña, J.M. Mapping crop calendar events and phenology-related metrics at the parcel level by object-based image analysis (OBIA) of MODIS-NDVI Time-Series: A case study Central California. *Remote Sens.* **2018**, *10*, 1745. [CrossRef]
77. Ali, A.; Rondelli, V.; Martelli, R.; Falsone, G.; Lupia, F.; Barbanti, L. Management zones delineation through clustering techniques based on soils traits, NDVI data, and multiple year crop yields. *Agriculture* **2022**, *12*, 231. [CrossRef]